J Korean Soc Ther Radiol Oncol 2003;21(2):158~166

Conceptual Source Design and Dosimetric Feasibility Study for Intravascular Treatment: A Proposal for Intensity Modulated Brachytherapy

Siyong Kim, Ph.D.*, Eunyoung Han, M.S.†, Jatinder R. Palta, Ph.D.*, and Sung W. Ha, M.D.‡

*Department of Radiation Oncology, University of Florida, USA, †Department of Radiological and Nuclear Engineering, University of Florida, USA, ‡Department of Therapeutic Radiology, Seoul National University College of Medicine, Seoul, Korea

Purpose: To propose a conceptual design of a novel source for intensity modulated brachytherapy.
Materials and Methods: The source design incorporates both radioactive and shielding materials (stainless steel or tungsten), to provide an asymmetric dose intensity in the azimuthal direction. The intensity modulated intravascular brachytherapy was performed by combining a series of dwell positions and times, distributed along the azimuthal coordinates. Two simple designs for the beta-emitting sources, with similar physical dimensions to a ^{90}Sr/Y Novoste Beat-Cath source, were considered in the dosimetric feasibility study. In the first design, the radioactive and materials each occupy half of the cylinder and in the second, the radioactive material occupies only a quater of the cylinder. The radial and azimuthal dose distributions around each source were calculated using the MCNP Monte Carlo code.
Results: The preliminary hypothetical simulation and optimization results demonstrated the 87% difference between the maximum and minimum doses to the lumen wall, due to off-centering of the radiation source, could be reduced to less than 7% by optimizing the azimuthal dwell positions and times of the partially shielded intravascular brachytherapy sources.
Conclusion: The novel brachytherapy source design, and conceptual source delivery system, proposed in this study show promising dosimetric characteristics for the realization of intensity modulated brachytherapy in intravascular treatment. Further development of this concept will center on building a delivery system that can precisely control the angular motion of a radiation source in a small-diameter catheter.

Key Words: Intensity modulation, Intravascular brachytherapy, MCNP

Introduction

Recently, intravascular brachytherapy has received considerable attention for the prevention of restenosis of both coronary and peripheral blood vessels. It has been shown that radiation can substantially reduce the problem of restenosis after angioplasty.[1~10] Several techniques have been developed for the delivery of low dose radiation to the site of restenosis. Two major approaches are a temporary implant using a catheter-based delivery system and a permanent implant using radioactive stents.[11] In a catheter-based delivery system, the radiation source is introduced to the proper position through a catheter; it stays there for the amount of time needed to deliver the prescribed dose to the target and then is retracted. A radioactive stent is permanently placed in the obstructed vessel in a permanent implant system. Both gamma and beta emitters have been used in catheter-based radiation delivery systems, whereas radioactive stents have primarily used beta emitters only.

Two major issues arise with the current systems. The first is the centering of the radiation source in the coronary vessel and the effect of off-centering on the dose distribution in catheter-

Submitted December 4, 2002 accepted April 4, 2003
Reprint request to Sung Whan Ha, Department of Therapeutic Radiology, Seoul National University College of Medicine, Seoul, Korea
Tel: +82-2-760-2524, Fax: +82-2-742-2073
E-mail: swha@snu.ac.kr

based radiation delivery systems. The effect of off-centering is significant for both photon and beta emitters because of the short distances to dose prescription points. The short range of beta particles in tissue further alters the resulting dose distribution with even a slight off-centering of the delivery catheter. Amols *et al* have shown that a centering offset of 0.5 mm within a 3 mm artery can cause a dose asymmetry by a factor that ranges from 2 to 3 for both beta-emitting (^{32}P and ^{90}Sr) and gamma-emitting (^{192}Ir) sources.[12] Radioactive liquid- filled balloons would appear to avoid off-centering issue by evenly distributing the liquid source within the balloon. However inflation of the balloon leads to restricted blood flow through the vessel, thus leading to ischemia and vessel spasms and thus negating the potential advantage. The recently introduced helical balloon has the advantage of having adequate source centering while allowing minimal blood flow. The second major issue involves the inhomogeneous composition and geometric asymmetry of an atherosclerotic plaque. A common assumption for radiation dose calculation and delivery in intravascular brachytherapy has been that the target consists of a homogeneous medium equivalent to water that is azimuthally symmetric with respect to the long axis of a source. Since a stenotic human blood vessel often is lined with atheromatous plaques of heterogeneous composition,[13~19] the radiation dose distribution delivered can be significantly different from that calculated or prescribed. Furthermore, the asymmetric distribution of residual plaques can create a more heterogeneous dose distribution. Such significant discrepancies in dose distribution can introduce relatively large uncertainties in the limits of the dose window for effective and safe application of intravascular brachytherapy, and consequently in the clinical evaluation of the efficacy of intravascular brachytherapy.

Currently, no radiation dose delivery system for intravascular brachytherapy completely overcomes the issues of dose asymmetry due to radiation source off-centering and the heterogeneous composition of an atheromatous plaque. We propose a concept for an intensity modulated brachytherapy delivery system that potentially solves dose asymmetry problems associated with existing intravascular brachytherapy delivery systems. The proposed system can provide an azimuthally asymmetric dose distribution using different combinations of source orientations and source dwell times. Source orientation and dwell times are optimized to deliver the desired dose distribution to an appropriate radiation target obtained from imaging devices such as an intra vessel ultrasound scan (IVUS).

Materials and Methods

1. Source design

Traditionally, sealed brachytherapy sources are designed to provide azimuthally symmetric dose distributions. In principle, symmetric sources cannot provide the heterogeneous radiation intensity that is required to produce an optimal dose distribution through the heterogeneous and asymmetric target that is fairly common in intravascular brachytherapy treatments. Based on this consideration, a design for a brachytherapy source, named the intensity modulation brachytherapy source (IMBS), is introduced. Unlike other sources, the brachytherapy source consists of two parts, a radioactive part in either one half (π in azimuthal angle) or one fourth ($1/2\,\pi$ in azimuthal angle) of the source and the shielding material in the remainder of the source (Fig. 1). An azimuthally asymmetric dose distribution can be obtained from this source by using different combinations of azimuthal source positions and source dwell times. Source positions and dwell times are optimized to deliver the desired dose distribution to an appropriate radiation target obtained from IVUS images. This source design can potentially be extended to other conventional brachytherapy applications.

2. Monte Carlo calculation

A Monte Carlo calculation is performed to obtain the dose distribution in water for the proposed brachytherapy source. A general-purpose photon/electron/neutron transport code developed at the Los Alamos National Laboratory (MCNP Version

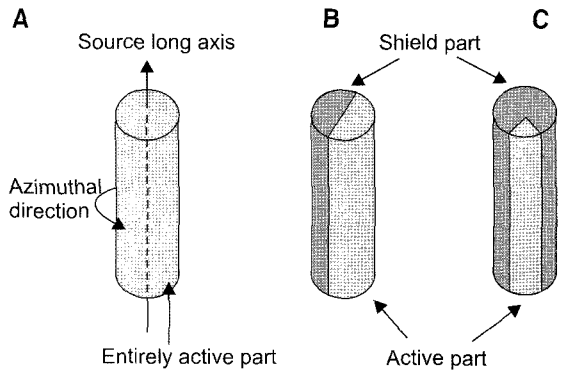

Fig. 1. General view of brachytherapy source: (**A**) conventional source-designed to give azimuthally symmetric dose distribution, (**B,C**) partially shielded source-designed to give azimuthally asymmetric dose distribution; dose optimization is obtained by optimizing dwell positions and dwell times.

4c) is used in this study. MCNP utilizes the condensed-history approach of Integrated Tiger Series (ITS) version 3.0 for electron transport.[20] MCNP has recently been used in medical physics as well as many other areas such as nuclear physics, nuclear engineering, and material science.

A ^{90}Sr/Y beta source that is similar to a Novoste Beta-Cath (Novoste Corporate, Norcross, GA, USA) source is assumed in this simulation. In the beta-cath system, the source is a cylindrical train of 12 or 16 source seeds, each having dimensions of 0.64 mm in diameter and 2.5 mm in length, and proximal/distal gold markers. Each seed contains ^{90}Sr/Y mixed with fired ceramic encapsulated in a 0.04 mm stainless steel wall. In this study, however, the source assumed is a cylinder having dimensions of 0.68 mm in outer diameter (including 0.04 mm thick stainless steel wall) and 2.5 mm in length. The calculation geometry is shown in Fig. 2. The calculation pixel was chosen in a cylindrical coordinate with radial interval of 0.2 mm and 10° azimuthal angle. The calculation was performed to 6 mm radial distance for only half of a circle because of the azimuthal symmetry. It is important to choose an appropriate shielding material to obtain an asymmetric dose distribution adequate for intensity modulation. Both stainless steel and tungsten were used in the computer simulation to determine which one provided the optimal shielding within the source size and geometric constraints. Emitting beta spectrum is simplified into 6 energy bins of 0.125, 0.25, 0.5, 1.5, 2.0, and 2.27 MeVs. Probabilities used for energy bins are 0.167, 0.158, 0.0875, 0.033, 0.01875, and 0.00625 respectively. Summarized is detail information for Monte Carlo calculation in Table 1. Bremsstrahlung x-ray production from the beta rays of the source is estimated to be insignificant. For 1 MeV electron (average energy of ^{90}Y is 934 keV), radiation yield in tungsten material is about 6%. In the one fourth of the radiation source case (x-ray production is higher in one fourth design than one half), we can assume 3 electrons enter into tungsten shield when 1 electron heads to non-shield direction. Conservatively assuming 100% of energy is absorbed within shield, x-ray production is approximately $3 \times 0.06 = 0.18$, that is, 18% of 1 electron energy heading to non-shield direction. If we assume an isotropic distribution of x-ray intensity, the energy fluence to each quadrant is 4.5%. Considering much longer penetration of x-rays compared to electrons, real energy deposition by x-rays is expected to be insignificant within the range of interest. Therefore, we have

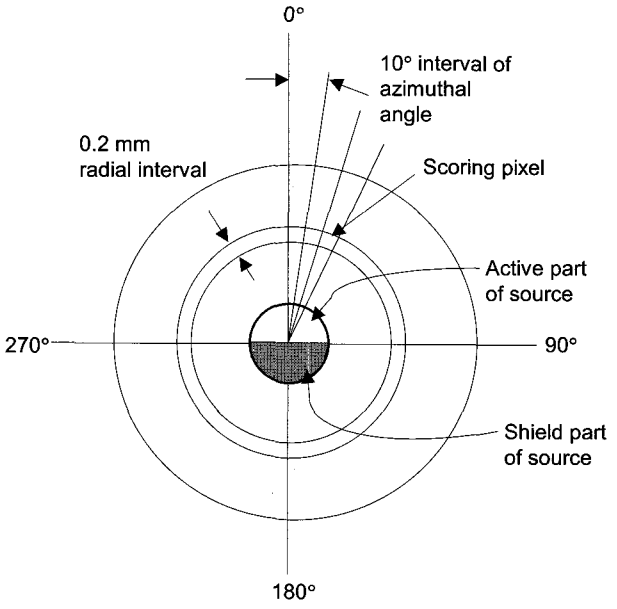

Fig. 2. MCNP calculation geometry.

Table 1. Parameters Used for MC Calculation

Mode	Spectrum		Material and weight fraction				History
	MeV	Probability	Water	Stainless steel	Tungsten	Al.Oxide	
Electron	0.125	0.167	H 0.11 O 0.89	Si 0.01 Cr 0.17 Mg 0.02 Fe 0.68 Ni 0.12	W 1.0	Al 0.71 O 0.89	6 million
	0.25	0.158					
	0.5	0.0875					
	1.5	0.033					
	2.0	0.01875					
	2.27	0.00625					

ignored the energy deposition by the bremsstrahlung x-rays in our analysis.

3. Dose optimization

As an example of dose optimization, we consider an off-center placement of a source. As shown in Fig. 3, the source is placed 0.75 mm off center in a 3 mm diameter vessel. Optimization is performed to provide a dose as uniform as possible at 2 mm distance from the center of the vessel. This is the recommended dose prescription point for the Novoste system. Dose optimizations should be performed in three-dimensional geometry. We, however, consider only a two-dimensional geometry for this feasibility test because dose contribution in longitudinal direction is relatively insignificant. In principle, a minimum of four dose calculation points (D_1, D_2, D_3, and D_4) are needed to obtain four dwell times (t_1, t_2, t_3, and t_4) as shown in Fig. 3, where t_j is the optimized dwell time for dwell position with which source part is heading to point j (j = 1, 2, 3, and 4). Therefore, the problem can be as simple as 4 linear equations with 4 unknowns like

$$D_i=\sum_{j=1,2,3,4} D_0\ R\ (\gamma_i)\ A\ (\gamma_i, \varphi_{ij})\ t_j \quad \text{for } i=1,\ 2,\ 3,\ \text{and } 4 \quad \cdots\cdots (1)$$

where

D_0=dose rate at radius of 1 mm through azimuthal angle 0°,

$R\ (\gamma)$=relative radial dose distribution at radius γ through azimuthal angle 0°,

γ_i=radius from the center of source to the dose calculation point i,

A (γ, φ)=azimuthal dose distribution at angle φ and radius γ, and

φ_{ij}=azimuthal angle between point i and the source with dwell position j.

Our problem can even be simplified further to 3 linear equations with 3 unknowns because of the symmetry of the geometry (i.e., $t_2 = t_3$). It may be possible to solve an inverse matrix directly when it is well conditioned. However, in practice, as the number of dwell positions increases, iterative methods can be applied. The optimization routine optimizes the dwell positions in the azimuthal direction. Intuitively, an optimal solution will result from an infinite number of dwell positions, but this is not practical. We arbitrarily constrained the optimization to four dwell positions for practical reasons.

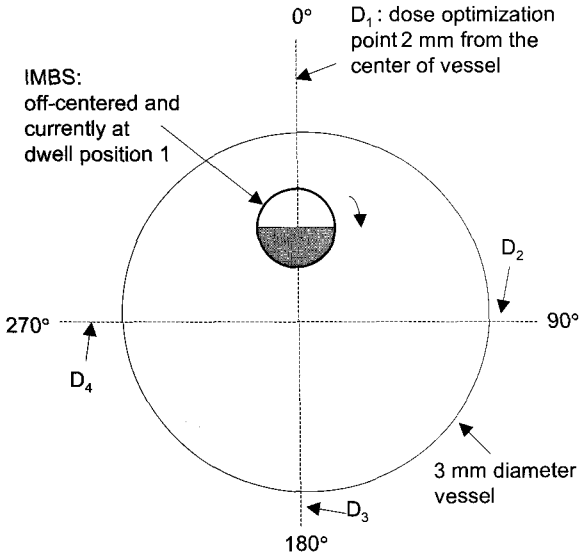

Fig. 3. Dose optimization geometry.

Results

1. Monte Carlo calculation

The relative dose distributions through azimuthal angle at a radius of 1, 2, 3, and 4 mm from the center of the source are shown in polar coordinates in Fig. 4 through 7. Results for a one-half-radioactive source (hereafter, we will call π source) with a stainless steel (SS) shield and a tungsten (W) shield are shown in Fig. 4 and 5, respectively. Fig. 6 and 7 show results for a one-fourth-radioactive source (hereafter, we will call 1/2 π source)

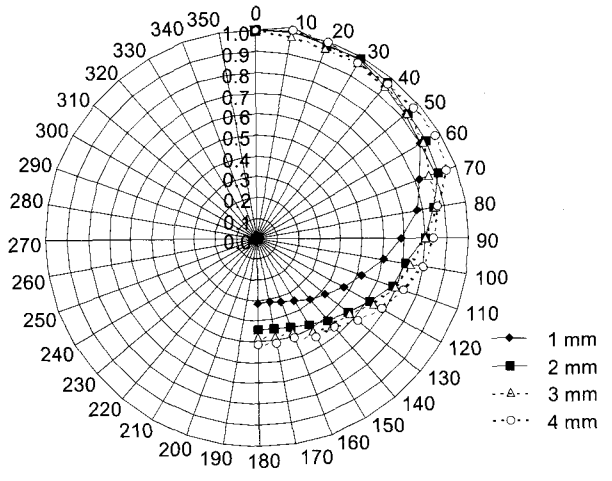

Fig. 4. Relative azimuthal dose distribution at bisector plane in polar coordinate by distances from the center of the source: π source with stainless steel shield.

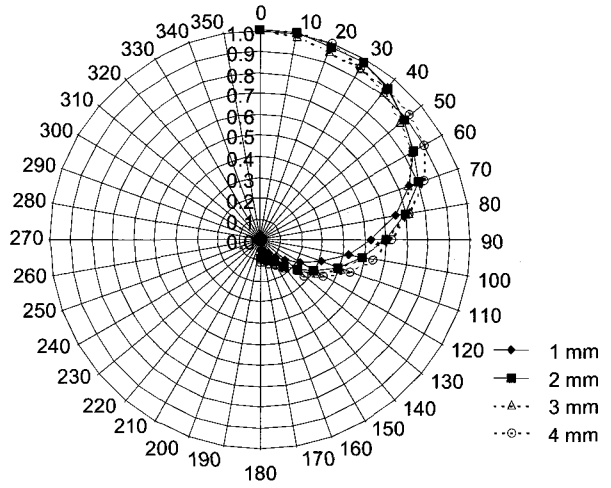

Fig. 5. Relative azimuthal dose distribution at bisector plane in polar coordinate by distances from the center of the source: π source with tungsten shield.

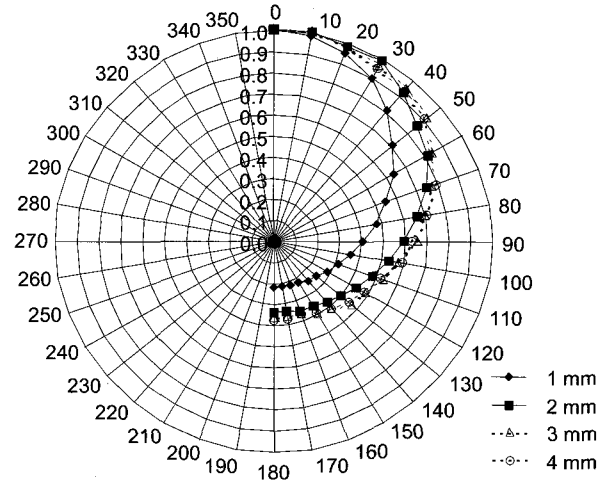

Fig. 6. Relative azimuthal dose distribution at bisector plane in polar coordinate by distances from the center of the source: $1/2\,\pi$ source with stainless steel shield.

with a stainless steel shield and a tungsten shield, respectively. Relative dose values are normalized to the dose value at 0°, where the dose rate is maximal at each radius. The degree of intensity modulation is dependent of the asymmetry of the azimuthal dose distribution for each shielded source. Therefore, it is useful to define a quantity, intensity modulability (*IM*), that is the ratio of the maximum and minimum dose rates. It is clear that a higher resolution of intensity modulation can be obtained with a higher *IM*. With an ideal shielding material, the minimum reaches to zero, thus resulting in a *IM* of infinity. We also define angular

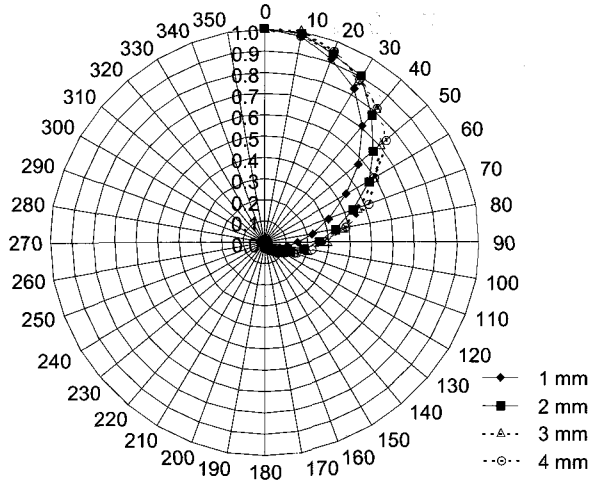

Fig. 7. Relative azimuthal dose distribution at bisector plane in polar coordinate by distances from the center of the source: $1/2\,\pi$ source with tungsten shield.

Table 2. Intensity Modulability and Angular Length: values are at radius of 1 mm

	IM	A_{80}	A_{50}	A_{20}
1/2 Source SS Shield	3.2	74	114	NA
1/2 Source W Shield	19.4	64	93	123
1/4 Source SS Shield	4.7	40	75	NA
1/4 Source W Shield	65.8	32	56	84

SS: stainless steel, W: tungsten

index (A_X), which is an angle where dose rate is X percent of the maximum. Apparently, we can use angular index to indicate a range of angles for which the dose rate is either significant or insignificant. For example, A_{80}=40° means dose distribution is equal to or higher than 80% of maximum between −40° (320) and 40°. It is expected that A_X can be correlated with an optimum number of dwell positions. On the other hand, A_{20}=150° indicates dose is equal to or lower than 20% in the range of 150° to 210° It is intuitive that an $1/2\,\pi$ source gives a higher *IM* than a π source does (refer to Fig. 4~7). It is also obvious that tungsten is a better shielding material compared with stainless steel because it provides better *IM*s. Table 2 summarizes *IM*, A_{80}, A_{50}, and A_{20} obtained at radius of 1 mm for each source design. Relative radial dose distributions are similar to each other for all four different source designs with slightly faster dose falloff for the $1/2\,\pi$source. Fig. 8 and 9 show relative radial dose distributions for the π and $1/2\,\pi$ source with tungsten shields, respectively. Polynomial equations were fitted to the calculated dose distri-

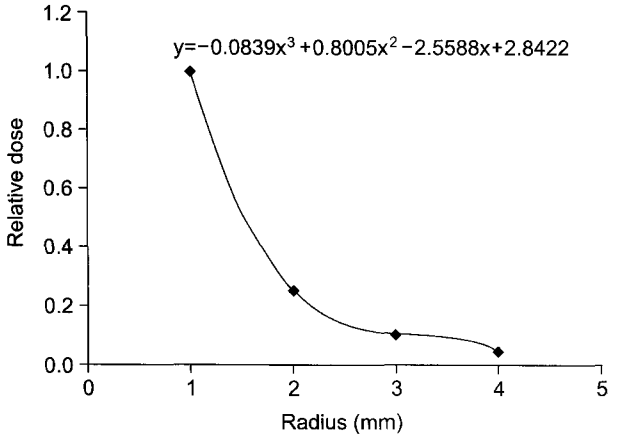

Fig. 8. Relative radial dose distribution at bisector plane: π source with tungsten shield. A polynomial-fitting equation is obtained for dose optimization with x=radial distance from the center and y=relative dose (dotted line).

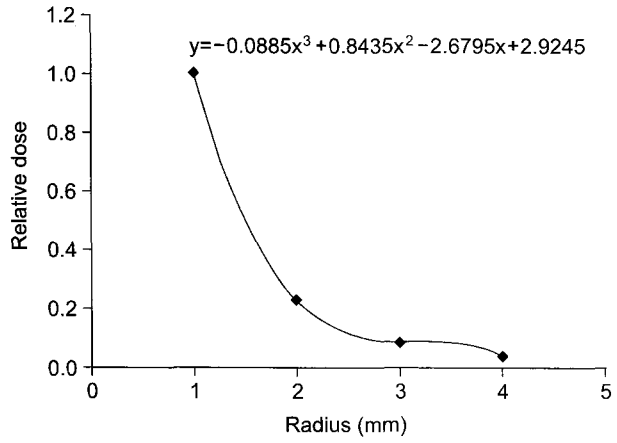

Fig. 9. Relative radial dose distribution at bisector plane: $1/2\pi$ source with tungsten shield. A polynomial-fitting equation is obtained for dose optimization with x=radial distance from the center and y=relative dose (dotted line).

butions and were used for dose optimization calculations. For dose optimization, azimuthal dose distributions also were fitted for the π and $1/2\pi$ source with tungsten shields (Fig. 10 and 11, respectively). Although the difference in the azimuthal dose distributions for the 1 mm and 2 mm radii is significant, the differences among 2, 3, and 4 mm radii are insignificant. Therefore, we obtained a single fitting equation for the dose optimization calculation that is representative of azimuthal dose distributions at radii 2 mm and greater from the center of the source.

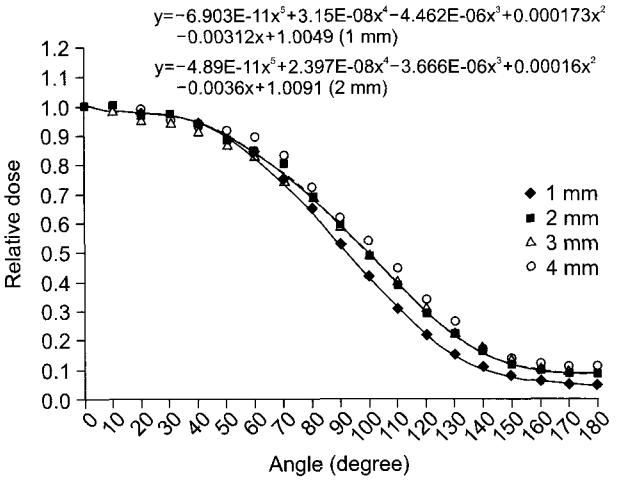

Fig. 10. Relative azimuthal dose distribution at bisector plane: π source with tungsten shield. Polynomial-fitting equations are obtained for dose optimization with x=azimuthal angle and y=relative dose (dotted lines).

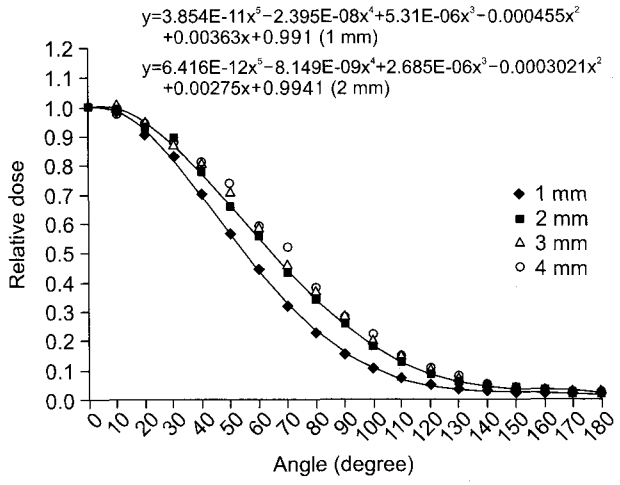

Fig. 11. Relative azimuthal dose distribution at bisector plane: $1/2\pi$ source with tungsten shield. Polynomial-fitting equations are obtained for dose optimization with x=azimuthal angle and y=relative dose (dotted lines).

2. Dose optimization

Optimized relative azimuthal dose distributions are shown in Fig. 12 and 13, respectively, for the π and $1/2\pi$ source with tungsten shields. Doses are calculated at 15° intervals using dwell times obtained through optimization. Values are normalized to the maximum. For comparison, dose distributions from a conventional source design that has uniform dose intensity in the azimuthal direction are also shown. It is very clear that IMBS

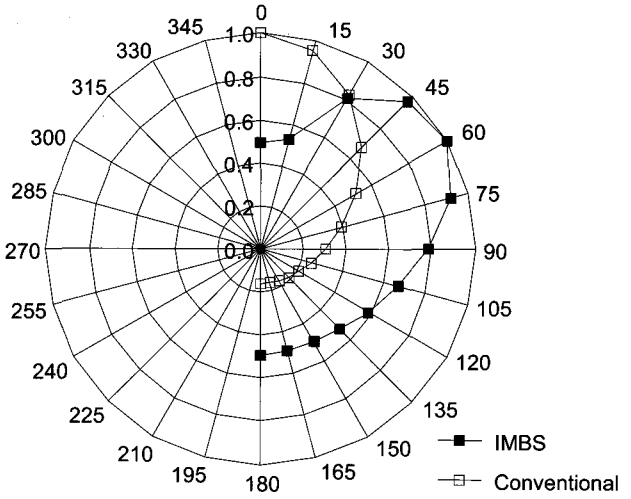

Fig. 12. Relative optimized azimuthal dose distribution at bi-sector plane in polar coordinate: π source with tungsten shield. Dose distribution with conventional source is also shown for comparison.

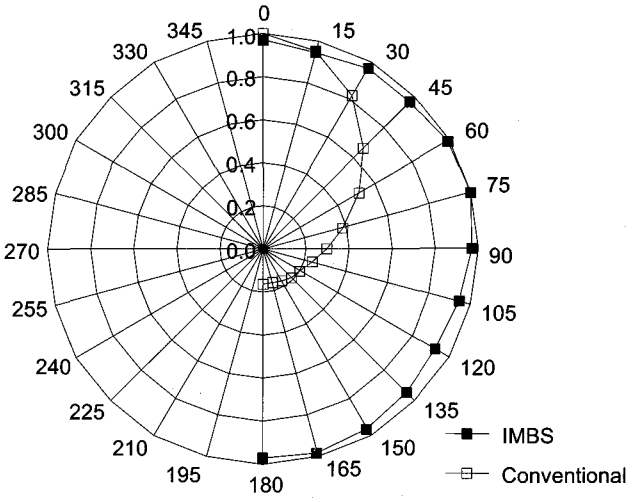

Fig. 13. Relative optimized azimuthal dose distribution at bi-sector plane in polar coordinate: $1/2\pi$ source with tungsten shield. Dose distribution with conventional source is also shown for comparison.

Table 3. Relative Optimized Dwell Times: normalized to t_1

	t_1	t_2	t_3	t_4
1/2 Source W Shield	1	0	11.57	0
1/4 Source W Shield	1	0.55	9.63	0.55

W: tungsten

provides a much improved dose distribution, especially the $1/2\pi$ source design. Compared with the minimum dose of 13% in conventional source design, IMBS gives 48% in the π source design and 93% in the $1/2\pi$ source design. Table 3 summarizes optimized relative dwell times. Whereas direct matrix inversion was achieved for the $1/2\pi$ source, a forward optimization was performed with the π source because a negative dwell time was obtained by the direct inverse method. As shown in Table 3, only two dwell positions, t_1 and t_2 have dwell times for the π source.

Discussion

We have considered only a two-dimensional geometry for this feasibility test. In a clinical situation, dose optimizations should be performed in three-dimensional geometry. Dose contribution from axial direction is rather close to 1/r fall off than $1/r^2$, which makes dose heterogeneity less severe in general. This, therefore, will make dose homogeneity slightly better. Three-dimensional optimization must also take into account the axial inhomogeneity in vessel cross-section, vessel curvature, dosimetric perturbation by plaque, and relative motion between the vessel and the source. Therefore, it is critically important to utilize IVUS images to obtain more accurate spatial information of clinical geometry. IVUS images can potentially provide data on source off-centering, geometry of vessel, plaque composition and thickness, and vessel motion. Three-dimensional dose optimization will be possible by stepping (axial direction) and rotation (radial direction) of the source. Treatment time can be a disadvantage of this method compared to current practice with beta source. However, when we consider the typical delivery time needed with ^{192}Ir source, it could be within a range reasonably acceptable. It can be reduced by optimal isotope, source length, and operating mechanisms.

Fabrication of IMB delivery system is a real challenge. We are considering mechanical approach currently. There are wires that can be rotated to certain degree without cranking even when it is located in a curved catheter. A test is on going to find how much and accurately control the angular rotation with several different wires. If that kind of wire is found, the source can be connected to the end of the wire and rotated clockwise 180° and counterclockwise 180°. Another possible approach is to use electrical control system. There are already a lot of electrical devices that require rotation within blood vessel (e.g., IVUS). Therefore, we believe, it will be possible to make an electrical device that can control the angular rotation of source. Electrical device will give higher precision but be more expensive.

The concept of IMB will not be restricted to intravascular therapy. This technique can be utilized for conventional brachytherapy as the image-guided brachytherapy becomes more important and popular. When it is combined with current remote after-loading technique like HDR (High Dose Rate) brachytherapy, IMB may be realized with relative ease. Uniformity of azimuthal dose distribution in intravascular brachytherapy can be improved enormously by intensity modulated brachytherapy (IMB). IMB can be performed with the shielded source design proposed in this paper and a delivery system (yet to be designed) that permits controlled angular rotation of this source around its own long axis. With such a system, optimized dose distribution can be delivered by a combination of dwell positions and dwell times in azimuthal coordinates. In a simple off-centering case, a conventional intravascular brachytherapy source delivers azimuthal dose distribution with an 87% difference between the maximum and the minimum dose to the lumen surface. This type of dose non- uniformity can be easily reduced to less than 7% with an intensity modulated brachytherapy source. The assumption is made here that the angular rotation of the source can be controlled.

This paper describes a novel brachytherapy source design and a conceptual source delivery system that has the potential to significantly improve dose uniformity in intravascular brachytherapy. Further development of this concept hinges on building a delivery system that precisely controls the angular motion of a radiation source in a small-diameter catheter. This is not completely out of the realm of reality as there are several electromechanical devices routinely used in microsurgery that have precision motion requirements much more stringent than those of the proposed intravascular brachytherapy delivery system. We have started some preliminary discussions with our electrical/biomedical engineering departments to build such a device. Other significant challenges include the interpretation of IVUS images for source off-centering, geometry of vessel, plaque composition and thickness, and vessel motion.

References

1. **Waksman R, King SB, Crocker IR, Mould RF.** Vascular Brachytherapy. Columbia, MD: Nucletron Corporation, 1996
2. **Waksman R, Robinson KA, Crocker IR, et al.** Intracoronary low dose beta irradiation inhibits neointima formation after coronary artery balloon injury in the swine restenosis model. Circulation 1995;92:3025-3031
3. **Waksman R, Robinson KA, Crocker IR, et al.** Intracoronary radiation prior to stent implantation inhibits neointima in stented porcine coronary arteries. Circulation 1995; 92:1383-1386
4. **Verin V, Popowski Y, Urban P, et al.** Intra-arterial beta irradiation prevents neointimal hyperplasia in a hypercholestrolemic rabbit restenosis model. Circulation 1995;92: 2284-2290
5. **Wiedermann JG, Marboe C, Amols H, Schwartz A, Weinberger J.** Intracoronary irradiation markedly reduces restenosis after balloon angioplasty in a porcine model. J Ameri Coll Cardio 1994;23:1491-1498
6. **Hehrlein C, Stintz M, Kinscherf R, et al.** Pure beta particle emitting stents inhibit neointima formation in rabbits. Circulation 1996;93:641-645
7. **Hehrlein C, Gollan C, Dönges K, et al.** Low-dose radioactive endovascular stents prevent smooth muscle cell proliferation and neointimal hyperplasia in rabbits. Circulation 1995;92:1570-1575
8. **Laird JR, Carter AJ, Kufs WM, et al.** Inhibition of neointimal proliferation with a beta particle emitting stent. Circulation 1996;93:529-536
9. **Carter AJ, Laird JR.** Experimental results with endovascular irradiation via a radioactive stent. Int J Radiat Oncol Biol Phys 1996;36:797-803
10. **Fischell TA, Carter AJ, Laird JR.** The beta-particle-emitting radioisotope stent (Isostent): animal studies and planned clinical trials. Am J Cardiol 1996;78:45-50
11. **Nath R, Almos H, Coffey C, et al.** Intravascular brachytherapy physics: Report of the AAPM Radiation Therapy Committee Task Group No. 60. Med Phys 1999;26:119-152
12. **Amols HI, Zaider M, Weinberger J, et al.** Dosimetric considerations for catheter based beta and gamma emitters in the therapy of neointimal hyperplasia in human coronary arteries. Int J Radiat Onc Biol Phys 1996;36:913-921
13. **Wexler L, Brundage Brouse J, Detrano R, et al.** Coronary artery calcification: pathophysiology, epidermiology, imaging methods, and clinical implications: a statement for health professionals from the American Heart Association. Circulation 1996;94:1175-1192
14. **Hatsukami TS, Ferguson MS, Beach KW, et al.** Carotid plaque morphology and clinical events. Stroke 1997;28:95-100
15. **Hatsukami TS, Thackray BD, Primozich JF, et al.** Echolucent regions in carotid plaque: preliminary analysis comparing three-dimensional histologic reconstructions to sonographic findings. Ultrasound Med Biol 1994;20:743-749
16. **Porter TR, Radio SJ, Anderson JA, et al.** Composition of coronary atherosclerotic plaque in the intima and media affects intravascular ultrasound measurements of intimal thickness. J Am Coll Cardiol 1994;23:1079-1084
17. **Mazzone AM, Urbani MP, Picano E, et al.** In vivo ultrasonic parametric imaging of carotid atherosclerotic plaque by videodensitometric technique. Angiology 1995;46:663-672
18. **Beletsly VY, Lelley RE, Fowler M, et al.** Ultrasound

densitometric analysis of carotid plaque composition: Patho-anatomic correlation. Stroke 1966;27:2173-2177

19. **Londero HF, Laguens R, Telayna JM, et al.** Densitometric quantitative analysis of intracoronary ultrasound images: anatomopathological correlation. Int J Card Imaging 1977;13:125-132

20. **Briesmeister JF, Editor, MCNP™.** A General Monte Carlo N-Particle Transport Code. Los Alamos National Laboratory report LA-13709-M. April, 2000

국문초록

혈관내 방사선치료를 위한 이론적 선원 설계 및 선량적 관점에서의 적합성 연구: 출력변조를 이용한 근접치료에 대한 제안

Florida 대학교 방사선종양학과*, 방사선-원자력공학과†,
서울대학교 의과대학 치료방사선과학교실†

김시용* · 한은영† · Jatinder R. Palta* · 하성환†

목 적: 본 연구는 새로운 근접치료선원의 이론적 설계를 통해 출력변조를 이용한 혈관내 방사선치료를 제안한다.

대상 및 방법: 제시된 이론적 선원은 기존의 선원과는 달리 선원물질과 차폐물질(스테인리스 스틸, 또는 텅스텐) 둘 다로 구성되며 이는 방위방향으로 비대칭적 방사선량을 제공할 수 있게 한다. 따라서, 방위방향으로 선원의 방향과 체류시간을 조절함으로써 출력변조를 통한 근접치료가 가능해진다. Novoste Beta-Cath system에서 사용하는 Sr-90/Y 전자방출 선원과 유사한 모양의 두 가지 단순화한 선원을 연구의 대상으로 고려하였다. 첫 번째 선원은 선원물질과 차폐물질이 각각 반씩 차지하며, 두 번째 선원은 1/4은 선원물질로, 나머지 3/4은 차폐물질로 구성된다. 두 선원에 대해 방위 및 방사방향으로의 선량분포를 MCNP 몬테 카를로 코드를 이용하여 계산하였다.

결 과: 선원이 혈관내의 중심에 위치하지 않게 되는 가상조건에서의 선량 최적화 계산을 시도한 결과, 혈관내벽에 미치는 선량의 최고치와 최저치의 차이가 87%에서 7%까지 줄어들 수 있음을 보였다.

결 론: 본 연구에서 제시된 이론적 선원은 선량적 관점에서의 적합성 여부에 관해 매우 고무적인 결과를 보여 줌으로써 출력변조를 통한 혈관내 근접방사선치료의 가능성을 나타내었다. 본 과제의 다음 단계는 굵기가 가는 맥관 내에서 선원의 위치를 파악하여 그를 방위방향으로 정확하게 회전시킬 수 있는 방사선 전달 체계의 개발이라 할 수 있다.

핵심용어: 출력변조, 혈관내 근접치료, MCNP